

but with significantly larger means, 53 and 206 ms ($n = 206$ events). A quantitative expression of channel activation by InsP_3 and blockade by nitrendipine is given in Fig. 2c, d. The probability of finding one or more open channels as a function of time was calculated every 250 ms for a total period of 40 s before addition of InsP_3 (trace 1), after channel activation by $10 \mu\text{M}$ InsP_3 (trace 2) and after blockade by $20 \mu\text{M}$ nitrendipine (trace 3). In c, the open probability during each consecutive period of 250 ms is plotted as a bar of magnitude 0 to 1. In Fig. 2d, the same experiment is plotted as the cumulative sum of probabilities in each period. A straight line in Fig. 2d would indicate a level of channel activation in which the nP_o product is invariant with time where n is the number of channels and P_o is the open probability. The trace 2 in Fig. 2c, d indicates that this was roughly so. In eight cases analysed InsP_3 induced a stationary open probability that remained constant for up to 240 s, the longest monitoring period. Hence InsP_3 channels do not inactivate with time. The average probability of one or more open channels (per 250 ms period) was $P_o = 0.014$ ($n = 8$) for $10 \mu\text{M}$ InsP_3 , $P_o = 0.035$ for $1 \mu\text{M}$ Bay K8644 ($n = 4$) and $P_o = 0.145$ ($n = 2$) for both added together which indicates a possible synergism of the two activators. The level of activity in trace 2 compared to that of trace 3 indicates that $20 \mu\text{M}$ nitrendipine blocked InsP_3 channels by approximately 10-fold.

Three separate results suggest that in the t-tubule preparation of skeletal muscle, the Ca^{2+} channel activated by Bay K8644 is the same as that independently activated by InsP_3 . (1) Both channels have a unit conductance of 10 pS in 100 mM Ba^{2+} and a selectivity $P_{\text{Ba}}/P_{\text{Na}} > 20$; (2) $20 \mu\text{M}$ nitrendipine blocks InsP_3 -activated and Bay K8644-activated channels; (3) in the absence of divalent ions in solution, the InsP_3 channel is permeable to Na^+ ions. We have made the same observation in dihydropyridine Ca^{2+} channels^{6,7}. In control experiments $10 \mu\text{M}$ inositol, inositol 1-phosphate, or inositol 1,2-cyclic phosphate, or incubation of vesicles for one hour with 1 mM MgATP failed to activate Ca^{2+} channels. However, the waiting time until channels were activated by InsP_3 was considerably reduced after incubation with MgATP. Also inositol 1,4-bisphosphate could replace InsP_3 in MgATP-treated vesicles, which probably reflects an effect of inositol 1,4-bisphosphate at some intermediary step of the phosphoinositide cascade. Inositol, inositol 1-phosphate or inositol 1,2-cyclic phosphate were ineffective in the presence or absence of MgATP. The fact that InsP_3 had an agonist effect at an 'infinite' dilution of cellular components, and in extremely simplified ionic solutions, is good evidence for a direct effect of InsP_3 on the Ca^{2+} channel. As the channel is inserted in a synthetic membrane that has an area roughly five orders of magnitude larger than a single t-tubule vesicle, all components present in the vesicle that fuses into the planar bilayer, would be immensely diluted into a vast excess of exogenous lipid. It is therefore very unlikely that if InsP_3 acted indirectly through an intermediary receptor, this receptor would in turn be able to locate the channel in the plane of the membrane. The large volume of the chamber in contact with the channel (3 ml on either side) helps eliminate the possibility that InsP_3 may be generating a diffusible activator.

Recent evidence indicates that the dihydropyridine receptor of skeletal muscle may have a dual function: as a Ca^{2+} channel^{19,20}, and as a voltage sensor of t-tubule depolarization responsible for triggering SR Ca^{2+} release²¹. It is also likely that InsP_3 may have several loci of action in excitation-contraction coupling, including that of putative second messenger¹⁸. All our evidence for InsP_3 activation of the Ca^{2+} release channel of rabbit skeletal muscle SR is negative however, and so we suggest that the site of action of InsP_3 in skeletal muscle is either the tubular membrane or the t-tubule/SR junction but not the SR membrane directly. This conclusion is directly supported by the work of Hannon and colleagues¹⁷, which first suggested that InsP_3 could open channels present in the transverse tubular membrane. Finally, the fact that InsP_3 opens Ca^{2+} channels at

0 mV is strong evidence in favour of a shift from inactivated-to-rest states or inactivated-to-open states. Otherwise, we would have not been able to record openings at depolarized potentials as all Ca^{2+} channels are inactivated at the time of membrane fractionation and purification. We suggest that InsP_3 could primarily facilitate the switching of channels away from the inactive state thus serving as an 'endogenous modulator'. Our data show that InsP_3 can mimic the dihydropyridine agonist Bay K8644 by directly opening Ca^{2+} channels although we do not know whether *in vivo* conditions favour this direct agonist effect.

This work was supported by NIH, Grants in Aid from the American Heart Association and the Muscular Dystrophy Association of America and by an Established Investigatorship from the American Heart Association to R.C.

Received 13 May; accepted 31 October 1988

- Berridge, M. *J. exp. Biol.* **124**, 323-335 (1986).
- Berridge, M. *A. Rev. Biochem.* **56**, 159-193 (1987).
- Vergara, J., Tsien, R. Y. & Delay, M. *Proc. natn. Acad. Sci. U.S.A.* **82**, 6352-6356 (1985).
- Volpe, P., Salvati, G., Di Virgilio, F. & Pozzan, T. *Nature* **316**, 347-349 (1985).
- Affolter, H. & Coronado, R. *Biophys. J.* **48**, 341-347 (1985).
- Coronado, R. & Affolter, H. *J. gen. Physiol.* **87**, 933-953 (1986).
- Coronado, R. & Smith, J. S. *Biophys. J.* **51**, 497-502 (1987).
- Ma, J. & Coronado, R. *Biophys. J.* **53**, 387-395 (1988).
- Valdivia, H. & Coronado, R. *Biophys. J.* **53**, 555a (1988).
- Vilven, J. *et al. Biophys. J.* **53**, 665a (1988).
- Lea, T. J., Griffiths, P. J., Treagear, R. T. & Ashley, C. C. *FEBS Lett.* **207**, 153-161 (1986).
- Nosek, T., Williams, M., Zeigler, S. & Godt, R. *Am. J. Physiol.* **19**, C807-C811 (1986).
- Walker, J. W., Somlyo, A. V., Goldman, Y. E., Somlyo, A. P. & Trentham, D. R. *Nature* **327**, 249-252 (1987).
- Rojas, E., Nassar-Gentina, V., Luxoro, M., Pollard, M. E. & Carrasco, M. A. *Can. J. Physiol. Pharmacol.* **65**, 672-680 (1987).
- Mikos, G. J. & Snow, T. R. *FEBS Lett.* **927**, 256-260 (1987).
- Donaldson, S. K., Goldberg, N. D., Walseth, T. F. & Huettman, D. A. *Proc. natn. Acad. Sci. U.S.A.* **85**, 5749-5753 (1988).
- Hannon, J. D., Lee, N. K. M. & Blinks, J. R. *Biophys. J.* **53**, 607a (1988).
- Suarez-Isola, B. A. *et al. Biophys. J.* **54**, 737-740 (1988).
- Flockerzi, V. *et al. Nature* **323**, 66-68 (1986).
- Smith, J. S. *et al. Biochem.* **26**, 7182-7188 (1987).
- Rios, E. & Brum, G. *Nature* **325**, 717-720 (1987).

A voltage-dependent chloride channel in the photosynthetic membrane of a higher plant

G. Schönknecht*, R. Hedrich, W. Junge* & K. Raschke

Pflanzenphysiologisches Institut, Universität Göttingen, D-3400 Göttingen, FRG

Photophosphorylation in photosynthetic membranes of plants (thylakoid membranes) is driven by an electrochemical potential difference of the proton¹. The light-driven net uptake of protons into the thylakoid lumen is electrically balanced by the motion of other ions^{2,3}. So far no ion channel has been identified in thylakoids other than the proton channel of the ATP synthase⁴ although charge balance would call for one. Patch-clamp studies⁵ on isolated membrane patches from osmotically inflated thylakoids of *Peperomia metallica* revealed a voltage-dependent and anion-selective channel. At 30 mM $[\text{Cl}^-]$ the single-channel conductance was 65 pS, showing ohmic behaviour between -80 and +80 mV. The opening probability was maximal at about +40 mV (inside the thylakoid). Application of voltage steps caused additional superimposed transient channel openings. This chloride channel could provide a mechanism involved in charge-balancing during light-driven proton uptake by thylakoids.

As in previous experiments with impalement microelectrodes^{6,7} giant chloroplasts of *P. metallica* were used. Proto-plasts

* Permanent address: Biophysik, FB Biologie/Chemie, Universität Osnabrück, D-4500 Osnabrück, FRG.

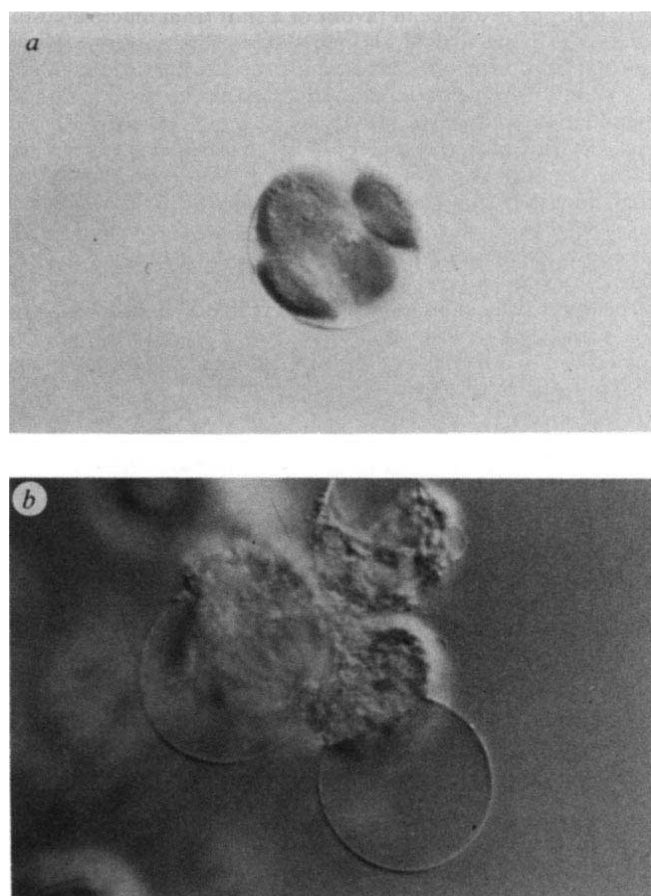


Fig. 1 Light microscopy (Nomarski interference contrast) of *a*, a protoplast (30 μm in diameter) and *b*, osmotically swollen thylakoids ('blebs'; same scale) of *Peperomia metallica*.

Methods. Leaf slices were incubated in 2% cellulase Onozuka R-10 and 1% Mazerocyme R-10 (Yakult Honsha, Tokyo, Japan), 0.5% bovine serum albumin, 0.27 M sorbitol, 1 mM CaCl_2 for about 1 h. Protoplasts were washed with 0.35 M sorbitol, 1 mM CaCl_2 , and separated from debris by filtration through 200- μm and 25- μm nylon nets followed by centrifugation, 7 min at 100g. The protoplasts were suspended in wash medium, stored on ice and used within 4 h. Protoplast suspensions (5–10 μl) were rapidly mixed with a 100-fold volume of bath solution (20 mM KCl, 5 mM MgCl_2 , 2 mM MOPS-KOH, pH 6.9 (MOPS is 3-(N-morpholino) propanesulphonic acid)) in the recording chamber⁹. After 15 min of osmotic swelling in the dark, plasma membranes, vacuoles and thylakoid envelopes had ruptured and thylakoids formed large blebs. The chamber was perfused with bath solution and blebs adhering to the bottom of the chamber were used for patch-clamp studies. All experiments were performed in 20 mM KCl, 5 mM MgCl_2 , 2 mM MOPS-KOH, pH 6.9 inside the pipette plus 1 mM CaCl_2 , unless indicated otherwise. Solutions were changed by bath perfusion.

were isolated from leaves (Fig. 1*a*) and osmotically shocked. This caused the rupture of the plasma membrane, the vacuole and the chloroplast envelope. Within 15 min of incubation several thylakoids were swollen to form large spherical membrane vesicles ('blebs') with up to 40 μm diameter (Fig. 1*b*). The thylakoid origin of the bleb membrane has been established by chlorophyll fluorescence, photochemical redox reactions sensitive to external electric fields⁸, as well as by light-driven⁹ and electric field-driven ATP synthesis¹⁰.

High-resistance seals (>10 G Ω) were formed between the fire-polished tip of patch pipettes and thylakoid membranes. They allowed single-channel recordings either in the thylakoid-attached configuration or, after withdrawal of the pipette, in the inside-out patch configuration⁹ (with the intrathylakoid mem-

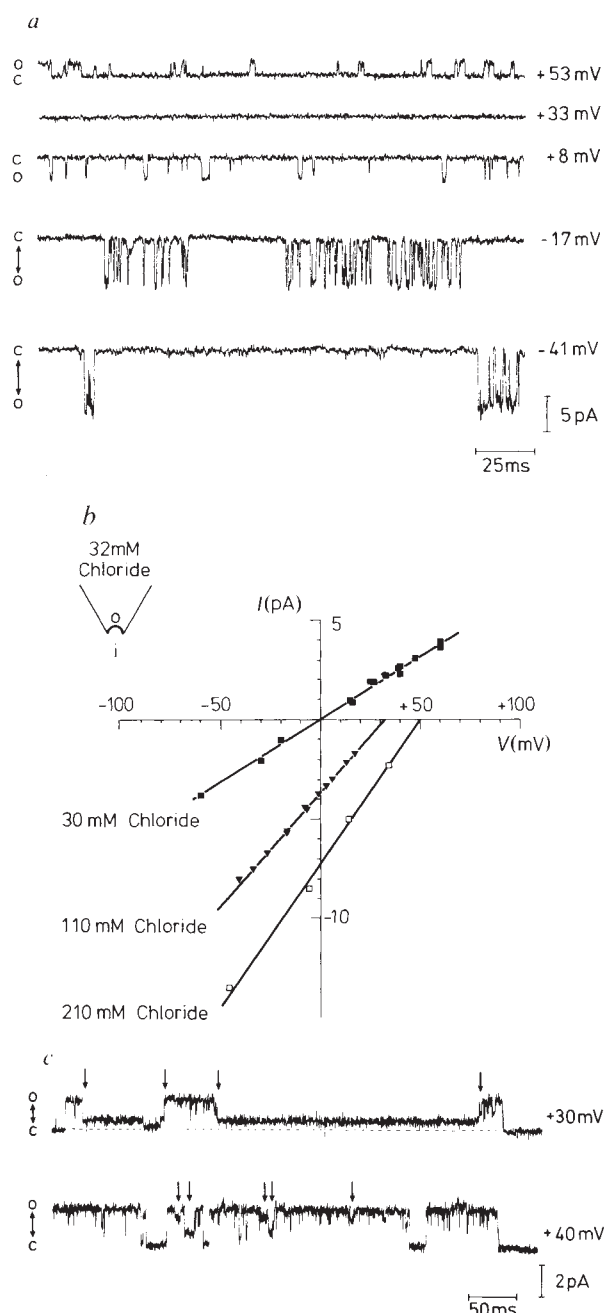
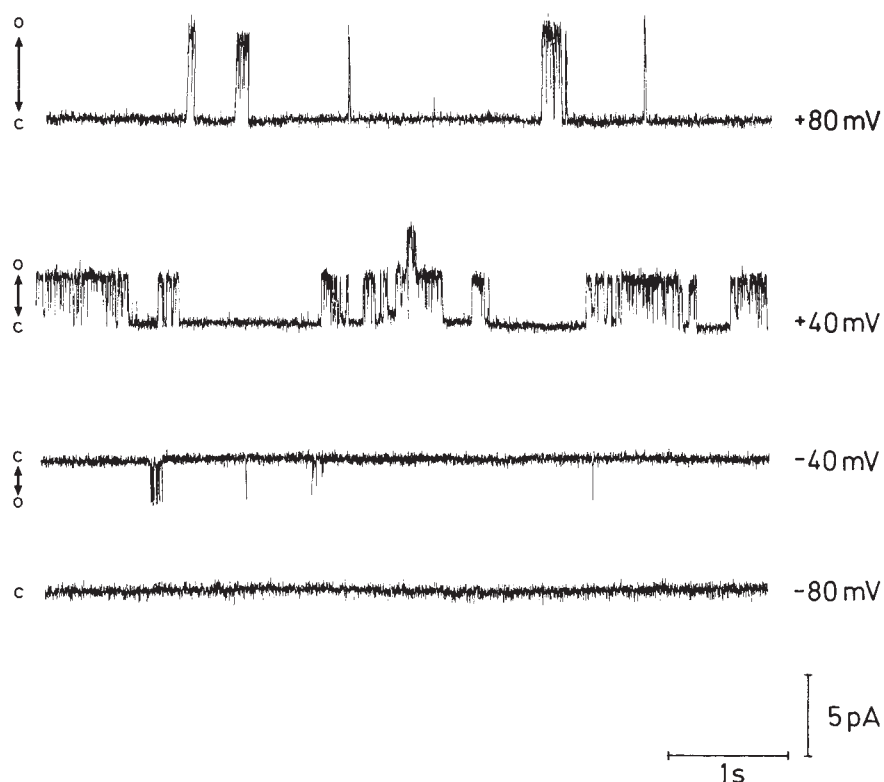


Fig. 2 Selectivity and current-voltage relationship of ion channels in the thylakoid. *a*, Single-channel recordings of chloride channels in inside-out patches (the intrathylakoid membrane side faced the bath solution) under asymmetrical KCl concentrations, 100 mM instead of 20 mM KCl in the bath. Upward current deflections represent Cl^- influx into the thylakoid, whereas downward deflections represent Cl^- efflux. *b*, Current-voltage relationships of the chloride channel at three different KCl gradients. Starting at 20 mM KCl, the concentration in the bath was raised to 100 or 200 mM KCl (background 5 mM MgCl_2 plus 1 mM CaCl_2 inside the pipette). The curves were fitted by linear regression. *c*, Subconductance levels of the chloride channel at holding potentials of +30 mV and +40 mV. All potentials given refer to the intrathylakoid side. **Methods.** Currents were recorded while the membrane potential was clamped to various positive or negative values or while double-voltage steps were applied. The first step, chosen to activate the channel (for example +40 mV; see Fig. 4), was followed by a second step to potentials at which the channel normally was closed. Membrane potentials and currents were measured with an EPC-7 patch-clamp amplifier (List Electronics), current records were stored on video tape, filtered at 2 kHz (8-pole Bessel characteristic) and analysed on a PDP 11/73 minicomputer.

Fig. 3 Voltage dependence of the chloride channel. The four current traces demonstrate representative channel activities, during 6-s time periods, when the potential was held at +80, +40, -40 or -80 mV.



brane face exposed to the bath). With a patch area of about $10 \mu\text{m}^2$ almost all patches contained at least one channel (and up to six, see Fig. 4a). When comparing attached configurations and inside-out patches no differences in single-channel behaviour were observed.

The ion selectivity was determined by the reversal of the single-channel currents in asymmetrical KCl solutions (Fig. 2a). The reversal potential followed the Nernst potential for chloride (Fig. 2b), as expected for an anion channel. Of the anions able to permeate thylakoid membranes¹¹ Cl^- is present in the chloroplast at the highest concentration. Thus the physiological role of this channel is that of a chloride channel.

Saturation of the single-channel conductance was observed by raising the Cl^- concentration on the intrathylakoid side (Fig. 2b): 30 mM, 65 ± 3 pS ($n = 14$); 110 mM, 110 ± 4 pS ($n = 4$); 210 mM, 141 pS and 126 pS. A maximal single-channel conductance of 150 pS and a Michaelis constant, K_m , for chloride of 40 mM were calculated, assuming Michaelis-Menten behaviour of the channel¹². The current-voltage relationship of the open channel was ohmic between +80 and -80 mV in symmetric and asymmetric KCl and KNO_3 solutions. Besides the main conductance state, subconductance levels were found (Fig. 2c), showing the same ion selectivity. Furthermore the thylakoid channel exhibited a complex gating behaviour, as the 'flickers' in Figs 2 and 4 demonstrate.

To determine the relative permeability for NO_3^- with respect to Cl^- , the reversal of the single-channel current was measured by replacing KCl by KNO_3 in the bath. The reversal potential shifted to positive values (data not shown), indicating a slightly higher permeability for NO_3^- than for Cl^- , as was reported for chloride channels in animal tissues¹³. Single-channel currents were about 25% higher in the presence of NO_3^- than in the presence of Cl^- .

Continuous illumination of thylakoids acidifies the lumen by about 3 pH units, we found however that variation of pH (between 7.8 and 5.9) at the intrathylakoid side affected neither the single-channel conductance nor the reversal potential.

Highest channel activity (under voltage-clamp) was observed at about +40 mV (inside the thylakoid). The activity decreased

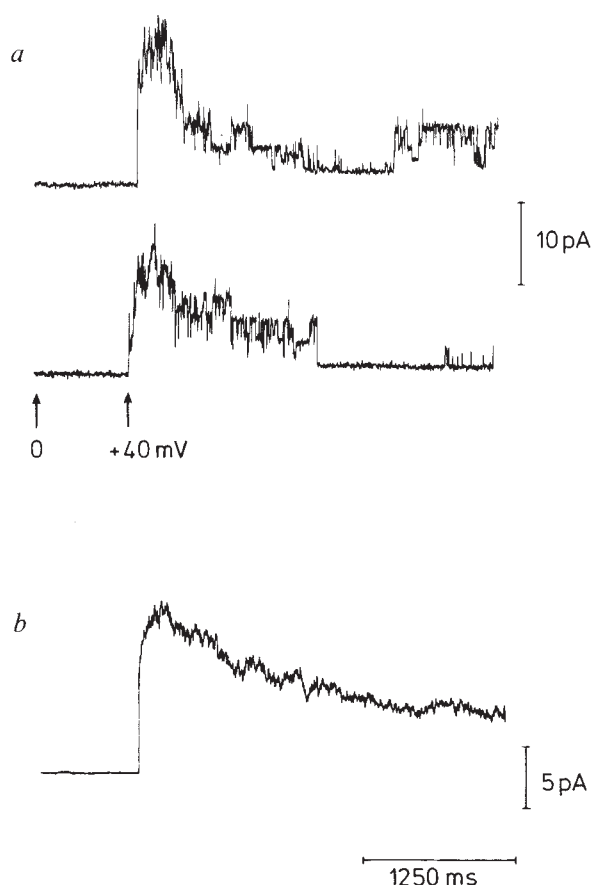


Fig. 4 Single-channel kinetics in response to voltage-step protocols. *a*, From a holding potential of 0 mV the potential was repetitively stepped to +40 mV for 3 s. With the onset of the +40-mV pulse single-channel activity rapidly increased (up to six channels opening simultaneously), followed by a slow decay to a steady state level. *b*, Average of 28 traces as shown in *a*.

as voltages were lowered or raised from +40 mV (Fig. 3). Changes of the holding potential to positive or negative values elicited additional channel openings. Transient channel openings were most pronounced at voltage steps to +40 mV (Fig. 4), a membrane potential comparable to that caused by a single light flash^{3,6}. From the average of 28 traces a half-rise time of less than 100 ms and a half-decay time of about one second were estimated. Generally, channel activity declined within 15–30 min after seal formation.

A voltage-dependent ion channel has been characterized recently in the inner mitochondrial membrane¹⁴. This channel had a similar conductance but was less anion selective than the thylakoid channel.

Because of the complex gating behaviour (sub-levels, flickers) and the decline of channel activity with time, it was not yet possible to study the kinetic properties of the Cl⁻ channel in thylakoids in more detail.

Earlier studies on passive ion movements associated with light-induced proton uptake into thylakoids gave rise to suggestions that electrical compensation was caused by Cl⁻ influx^{2,15}, or Mg²⁺ efflux¹⁶, or both¹⁷. We did not observe K⁺ or Mg²⁺ channels in solutions containing 5 mM MgCl₂ and up to 200 mM KCl. The described chloride channel would allow a rapid,

voltage-dependent uptake of Cl⁻ into thylakoids, and thus an electrical compensation of the light-driven proton uptake.

We thank I. Baumann for technical help, W. Lahr for support with computer software, B. Raufeisen for artwork, and W. Hanke, B. U. Keller and E. Neher for critical comments on the manuscript. Financial support was provided by the Deutsche Forschungsgemeinschaft.

Received 18 August; accepted 4 November 1988.

- Mitchell, P. *Biol. Rev.* **41**, 445–502 (1966).
- Rottenberg, H., Grunwald, T. & Avron, M. *Eur. J. Biochem.* **25**, 54–63 (1975).
- Junge, W. *Curr. Top. Membranes Transp.* **16**, 431–465 (1982).
- Lill, H., Althoff, G. & Junge, W. *J. Membrane Biol.* **98**, 69–78 (1987).
- Hamill, O. P., Marty, A., Neher, E., Sakmann, B. & Sigworth, F. J. *Pflügers Arch. ges. Physiol.* **391**, 85–100 (1980).
- Vredenberg, W. J. *Proc. 3rd Int. Congr. Photosynthesis* 929–939 (1974).
- Bulychev, A. A., Andrianov, V. K., Kurella, G. A. & Litvin, F. F. *Nature* **236**, 175–176 (1972).
- DeGrooth, B. G. & van Gorkom, H. J. *Biochim. biophys. Acta* **35**, 445–456 (1981).
- Campo, M. L. & Tedeschi, H. *Eur. J. Biochem.* **149**, 511–516 (1985).
- Gräber, P., Schlodder, E. & Witt, H. T. *Biochim. biophys. Acta* **461**, 426–440 (1977).
- Schuldiner, S. & Avron, M. *Eur. J. Biochem.* **19**, 227–231 (1971).
- Läuger, P. *Biochim. biophys. Acta* **311**, 423–441 (1973).
- Bormann, J., Hamill, O. P. & Sakmann, B. *J. Physiol.* **385**, 243–286 (1987).
- Sorgato, M. C., Keller, B. U. & Stühmer, W. *Nature* **330**, 498–500 (1987).
- Vambutas, V. & Beattie, D. S. *Biochim. biophys. Acta* **893**, 69–74 (1987).
- Chow, W. S., Wagner, G. & Hope, A. B. *Austr. J. Pl. Physiol.* **3**, 853–861 (1976).
- Hind, G., Nakatani, H. Y. & Izawa, S. *Proc. natn. Acad. Sci. U.S.A.* **71**, 1484–1488 (1974).

The maternal mRNA Vg1 is correctly localized following injection into *Xenopus* oocytes

Joel K. Yisraeli & D. A. Melton

Department of Biochemistry and Molecular Biology, Harvard University, Cambridge, Massachusetts 02138, USA

The animal and vegetal ends of *Xenopus* oocytes have distinctly different developmental fates. At the molecular level, several maternal mRNAs have been isolated that are localized to either the animal or vegetal hemisphere¹. One of these mRNAs, Vg1, is distributed homogeneously throughout the cytoplasm of early-stage oocytes and gets localized during oogenesis to a tight shell at the vegetal cortex of middle and late-stage oocytes². We have

used an *in vitro* culture system to demonstrate that exogenous Vg1 mRNA injected into middle-stage, but not late-stage, oocytes gets localized in a similar fashion to the endogenous message. Furthermore, translation of Vg1 mRNA is not required for the localization of the message itself. These results show that the information necessary to interpret the animal-vegetal polarity in oocytes is present in the naked mRNA transcript.

To study the Vg1 mRNA localization process, it was first necessary to obtain an *in vitro* culture system in which endogenous Vg1 mRNA is localized. Previous studies showed that endogenous Vg1 mRNA begins to localize in mid-stage oocytes (stage III, 0.5–0.6 mm in diameter²). We cultured stage III oocytes *in vitro* in a medium that contains vitellogenin³, and observed morphological changes associated with oocyte growth and development. In addition, *in situ* hybridizations show that the endogenous Vg1 mRNA is uniformly distributed in the cytoplasm at the beginning of the culture period, and is significantly concentrated in the vegetal hemisphere after only three

Fig. 1 Localization of endogenous Vg1 mRNA in cultured oocytes. Stage III albino oocytes (0.55–0.6 mm in diameter) were cultured in either medium supplemented with 10% vitellogenin-containing frog serum ('medium')^{3,4} or in 1× modified Barth's saline-HEPES (MBSH 'saline') for the indicated times. These dark-field photographs show the location of Vg1 transcripts as revealed by *in situ* hybridization with an antisense Vg1 RNA probe. Albino oocytes were used because the pigment granules in wild-type oocytes are almost indistinguishable from white autoradiographic silver grains. The nucleus or germinal vesicle (gv) appears as a dark circle in some sections. Here, as throughout the paper, whenever albino oocytes are used the sections are oriented with the putative vegetal pole down. In these middle-stage oocytes, the gv has not yet migrated to the animal hemisphere, making orientation of these albino oocytes difficult. On average the oocytes in medium grew in diameter from 0.55 mm at time 0 to 0.7 mm by day 6; those in saline showed a negligible increase. The ring of grains around the sections shown for time 0 results from an emulsion stretching artefact and is easily distinguished from hybridization when observed under the microscope.

Methods. Dissected oocytes (0.55 mm in diameter) were cultured in a 96-well plate at 20 °C in a humidified chamber in either 1× MBSH or 0.5× Leibowitz medium supplemented with glutamine, insulin, nystatin, gentamycin and 10% vitellogenin-containing frog serum^{3,4}. Blood containing serum rich in vitellogenin was isolated from female frogs injected three weeks earlier with 0.4 ml of 10 mg ml⁻¹ estradiol (Sigma) suspended in 1,3-propanediol³. At the end of the incubation, oocytes were fixed, sectioned, and hybridized² using a T7-synthesized [³²P]labelled, antisense Vg1 RNA probe containing the entire coding sequence of Vg1. Exposure time was five days to two weeks.

